14 July 2000

ELSEVIER

Chemical Physics Letters 324 (2000) 466–474

CHEMICAL PHYSICS LETTERS

www.elsevier.nl/locate/cplett

On the effect of increasing the total angular momentum on Li + HF reactivity

Antonio Laganà [a,*], Alessandro Bolloni [a], Stefano Crocchianti [a], Gregory A. Parker [b]

[a] *Dipartimento di Chimica, Università di Perugia, Perugia, Italy*
[b] *Department of Physics and Astronomy, University of Oklahoma, Norman, OK, USA*

Received 27 March 2000; in final form 22 May 2000

Abstract

The effect of increasing the total angular momentum J on the value of the reaction probability has been investigated theoretically using exact quantum calculations. The contribution of higher J probabilities to the calculated value of the cross-section has been treated as a correction to its J-shifting model formulation. Two interesting features of the calculated cross-section have been evidenced in this way: (a) as more exact quantum contributions are added to the calculation, the agreement between theory and experiment improves; (b) the resonance structure characterizing low-energy probabilities survives the averaging over partial waves.

1. Introduction

In recent years, the progress in rigorous quantum approaches to chemical reactivity [1] has made impressive advances thanks also to the possibility of comparing calculations with measurements performed using molecular beam apparatuses [2]. However, it is still quite challenging, from the computational point of view, to apply exact quantum techniques to the treatment of three-atom reactions having a strongly bent transition state and a structured potential energy surface (PES). This is particularly difficult for reactions whose arrangement channels have significantly different mass and energy properties. In this case convergence of the reactive cross-section with the value of the total angular momentum quantum number J may be so slow to require calculations at J values of the order of 10^2. For this reason it is extremely important to find relationships tieing the value of the reactive probability calculated at low J values with that calculated at high J values.

A suitable prototype for three-atom reactions having a bent transition state is Li + HF for which various classical (QCT) [3–6] and reduced dimensionality quantum [7–10] studies have already been reported in the literature. This type of studies were converged with total angular momentum both for full dimensional QCT approaches and for reduced dimensionality quantum ones (in the case of the infinite order sudden (RIOS) method convergence is

* Corresponding author. Fax: +39-75-5855606; e-mail: lag@unipg.it

0009-2614/00/$ - see front matter
PII: S0009-2614(00)00651-5

checked against the value of the orbital angular momentum l).

This type of studies have evidenced interesting properties of the Li + HF reaction some of which are directly related to the experiment [11,12]. For these properties quasiclassical calculations [6] performed on the PES described in Ref. [13] fitted using bond order [14] polynomials to adjusted ab initio potential energy values of Refs. [15,16] have given satisfactory agreement. Among these properties are the reactive cross-section and its energy dependence as well as some product distributions and stereodynamic properties.

Quasiclassical calculations and reduced dimensionality quantum ones also led to results highlighting the dynamic nature of related reactive mechanisms like the increase of the cross-section with the decrease of the collision energy about the threshold and the decrease of reactivity with the increase of both the F and the H mass via a substitution with heavier isotopes [7,8].

Exact quantum calculations for the title reaction have already been reported in the literature for zero total angular momentum. For the first time they were reported in Ref. [17] and then in Ref. [13] where the PES used for the calculation is also described. These results were compared with those obtained from a time-dependent treatment in Ref. [18]. Starting from these zero total angular momentum results cross-sections [19] and stereodynamical properties [20–22] have been estimated. Quantum techniques have also been used for calculating $J = 0$ isotopic properties [23].

In this Letter we report results of exact quantum calculations for the title reaction at a few small values of J. Related reactive probabilities are compared in order to evaluate the effect of increasing the total angular momentum on the value of partial wave contributions to the reactive cross-section of the system. Results from different J values are also combined together to provide approximate estimates of the reactive cross-section.

The Letter is articulated as follows. In Section 2 the computational procedure for total angular momentum values larger than zero is described. In Section 3 quantum probabilities calculated at increasing values of the total angular momentum and related product distributions are illustrated. In Section 4 the effect of increasing the total angular momentum is discussed and a comparison with a model treatment is made.

2. J > 0 quantum calculations

Our calculations have been performed using a revised version [24] of the time-independent APH3D code based on hyperspherical APH coordinates [25,26]. APH3D is a numerical procedure that calculates atom–diatom quantum reactive probabilities by determining the time-independent partial wave of the system. Each nth partial wave $\Psi^{JMpn}(\rho,\theta,\chi)$ (for the sake of simplicity the arrangement label of χ is dropped) of parity p is determined by integrating the time-independent nuclear Schrödinger equation that in hyperspherical coordinates reads

$$\left[T_\rho + T_\mathrm{h} + T_\mathrm{r} + T_\mathrm{c} + V(\rho,\theta,\chi)\right]\Psi^{JMpn}(\rho,\theta,\chi) = E\Psi^{JMpn}(\rho,\theta,\chi) \quad (1)$$

where E is the total energy of the system. In Eq. (1) J is the eigenvalue of the total angular momentum, and M its projection on the z axis of the space fixed frame. The various terms of the Hamiltonian are

$$T_\rho = -\frac{\hbar^2}{2\mu\rho^5}\frac{\partial}{\partial\rho}\rho^5\frac{\partial}{\partial\rho},$$

$$T_\mathrm{h} = -\frac{\hbar^2}{2\mu\rho^2}\left(\frac{4}{\sin 2\theta}\frac{\partial}{\partial\theta}\sin 2\theta\frac{\partial}{\partial\theta} + \frac{1}{\sin^2\theta}\frac{\partial^2}{\partial\chi^2}\right),$$

$$T_\mathrm{r} = A(\rho,\theta)J_x^2 + B(\rho,\theta)J_y^2 + C(\rho,\theta)J_z^2,$$

and

$$T_\mathrm{c} = -\frac{i\hbar\cos\theta}{\mu\rho^2\sin^2\theta}J_y\frac{\partial}{\partial\chi},$$

depending upon the hyperradius ρ and the two hyperangles θ and χ (subscripts 'h', 'r' and 'c' stand for 'hypersphere', 'rotational', and 'Coriolis', respectively). The constants A, B and C are defined as $A^{-1}(\rho,\theta) = \mu\rho^2(1+\sin\theta)$, $B^{-1}(\rho,\theta) = 2\mu\rho^2\sin^2\theta$, and $C^{-1}(\rho,\theta) = \mu\rho^2(1-\sin\theta)$ with μ being the reduced mass of the system.

The partial wave $\Psi^{JMpn}(\rho,\theta,\chi)$ is usually expanded in terms of products of the Wigner rotation functions $\hat{D}^{Jp}_{\Lambda M}$ of the three Euler angles α, β and γ

times the surface functions $\Phi_{t\Lambda}^{Jp}$ of the two internal hyperangles θ and χ at fixed (ρ_ξ) value of ρ (the key scattering information is carried by the expansion coefficients $\psi_{t\Lambda}^{Jpn}(\rho)$):

$$\Psi^{JMpn} = 4\sum_{t,\Lambda} \rho^{-5/2}\psi_{t\Lambda}^{Jpn}(\rho)\Phi_{t\Lambda}^{Jp}(\theta,\chi;\rho_\xi) \times \hat{D}_{\Lambda M}^{Jp}(\alpha,\beta,\gamma). \quad (2)$$

The substitution of the expansion (2) in Eq. (1) and the averaging over angular coordinates leads to the following set of coupled differential equations:

$$\left[\frac{\partial^2}{\partial\rho^2} + \frac{2\mu E}{\hbar^2}\right]\psi_{t\Lambda}^{Jpn}(\rho) = \frac{2\mu}{\hbar^2}\sum_{t'\Lambda'}\left\langle \Phi_{t\Lambda}^{Jp}\hat{D}_{\Lambda M}^{Jp}|H_I|\Phi_{t'\Lambda'}^{Jp}\hat{D}_{\Lambda' M}^{Jp}\right\rangle\psi_{t'\Lambda'}^{Jpn}(\rho). \quad (3)$$

where the internal Hamiltonian H_I reads

$$H_I = T_h + T_r + T_c + \frac{15\hbar^2}{8\mu\rho^2} + V(\rho,\theta,\chi).$$

To carry out the integration of Eqs. (3) the hyperradius is segmented into several sectors (277 in our case) and the following eigenvalue problem in θ and χ

$$\left[T_h + \frac{15\hbar^2}{8\mu\rho_\xi^2} + \hbar^2 GJ(J+1) + \hbar^2 F\Lambda^2 + V(\rho_\xi,\theta,\chi) - \varepsilon_{t\Lambda}^{Jp}(\rho_\xi)\right]\Phi_{t\Lambda}^{Jp}(\theta,\chi;\rho_\xi) = 0 \quad (4)$$

with $G=(A+B)/2$ and $F=C-G$, is solved at the midpoint of each sector ξ using the analytic basis method [27]. To not repeat the calculation of the surface functions at each value of J, as suggested by Launay [28], one can perform it at a reference value $\bar{J}$ of the total angular momentum quantum number that ensures a proper behaviour of the surface functions. In this case the surface functions are calculated by solving the equation

$$\left[T_h + \frac{15\hbar^2}{8\mu\rho_\xi^2} + \hbar^2 G\bar{J}(\bar{J}+1) + \hbar^2 C\Lambda^2 + V(\rho_\xi,\theta,\chi) - \varepsilon_{t\Lambda}^{Jp}(\rho_\xi)\right]\Phi_{t\Lambda}^{Jp}(\theta,\chi;\rho_\xi) = 0. \quad (5)$$

Accordingly, the internal Hamiltonian H_I of Eqs. (3) is modified as

$$H_I = T_h + T_r + T_c + \frac{15\hbar^2}{8\mu\rho^2} + V(\rho,\theta,\chi) + \hbar^2 G\left[J(J+1) - \bar{J}(\bar{J}+1) - \Lambda^2\right].$$

The coupled differential equations (3) in ρ are integrated by propagating the solution as an **R** matrix (at the border between adjacent sectors the **R** matrix has to be mapped from one sector surface functions onto those of the new sector). At the asymptote, a further mapping of the solution into Delves and then into Jacobi coordinates is performed, boundary conditions are imposed and the elements of the scattering matrix **S** matrix are evaluated.

The APH3D computational procedure is highly demanding in terms of memory and computing times. For this reason, APH3D has been articulated as a sequence of programs. The first program (ABM) performs the computation of surface functions solving Eq. (4). The second program (LOGDER) integrates Eq. (5) for the desired number of energies. For both ABM and LOGDER programs significant efforts were paid in their parallelization using models based on a dynamic allocation of the work load [29,30].

LOGDER is followed by a series of smaller programs at the end of which the **S** matrix is worked out. From a proper summation of the square modulus of the **S** matrix elements one obtains averaged and detailed reactive probabilities.

3. Reaction probabilities

Reaction probabilities were computed from threshold up to a total energy E of 0.6 eV for values

of the total angular momentum quantum number J varying from 0 to 2. For $J = 0$ E was varied in steps of 0.001 eV. State selected (for zero initial vibrational number v and various values of the initial rotational number j) $J = 0$ reactive probabilities summed over all product rotational states are shown in Fig. 1 as solid lines for the different values of the product vibrational states v'. Corresponding $J = 1$ (crosses connected by dotted lines) and $J = 2$ (circles connected by dashed lines) state selected reactive probabilities are also given in Fig. 1. In the case of $J = 1$ and $J = 2$ calculations E was varied in steps of 0.01 eV. As shown by the figure (where, as already mentioned, probability plots for non-zero J values have a lower resolution than the $J = 0$ plots) average contributions to reaction are almost the same for all values of J. Occasionally, some values exhibit larger differences. This may be due to the fact that resonances occur at different energies when J varies and that the coarser grids have not the necessary resolution. As apparent from the figure, reaction products are prevalently channeled into $v' = 0$ and reactive probability has a maximum 0.4–0.5 eV irrespective of the value of the total angular momentum. The threshold value of total energy increases with the initial rotational state j since not the whole energy supplied as reactants' rotation is suitable to enhance reaction. The threshold value of total energy increases also with the product vibrational excitation and the maximum of the reactive probability (that

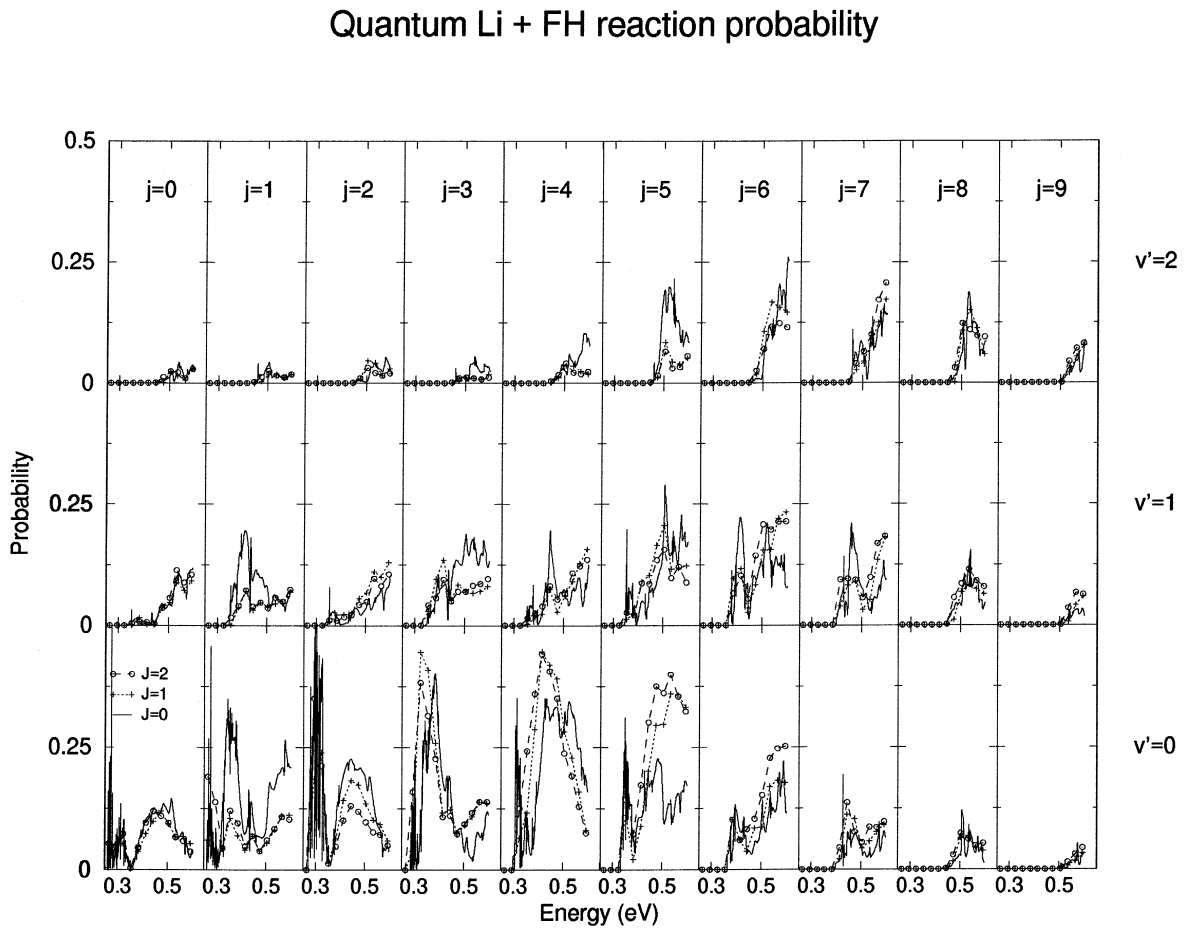

Fig. 1. Reactive probabilities summed over rotational product states (j') for single product vibrational states (v') calculated at $v = 0$ and at j values ranging from 0 to 9 (from lhs to rhs) for $J = 0$ (solid line), $J = 1$ (dotted line with crosses) and $J = 2$ (dashed line with circles) plotted as a function of total energy E.

becomes lower as v' increases) shifts to higher total energy with v'. A similar dependence from j is found when probabilities calculated at fixed value of v' are considered.

An evident feature of the $J = 0$ results (as it was shown by previous quantum calculations [13], for which a model rationalization was worked out, and confirmed by a stereodynamics study) is the combined action of two reaction mechanisms: A resonant-like mechanism dominant at low energy (responsible for probability spikes) and a more direct mechanism dominant at high energy (responsible for the smoother background signal). The trajectory study [31] depicted the indirect mechanism in terms of the formation of a weak triatomic aggregate in which H is gradually displaced before reaching a geometry leading to its expulsion and the direct mechanism in terms of an attack of Li on its final product partner F.

The dense quantum resonant structure superimposed to a background signal of the reactive probability of this reaction was rationalized in terms of bound states supported by the wells located at intermediate distances in the plots of the surface eigenvalues as a function of ρ. This resonance structure is particularly dense at low energy and persists when J increases.

The comparison has been extended also to the effect of the parity on the calculated probabilities. The two contributions (parity zero and one) to the

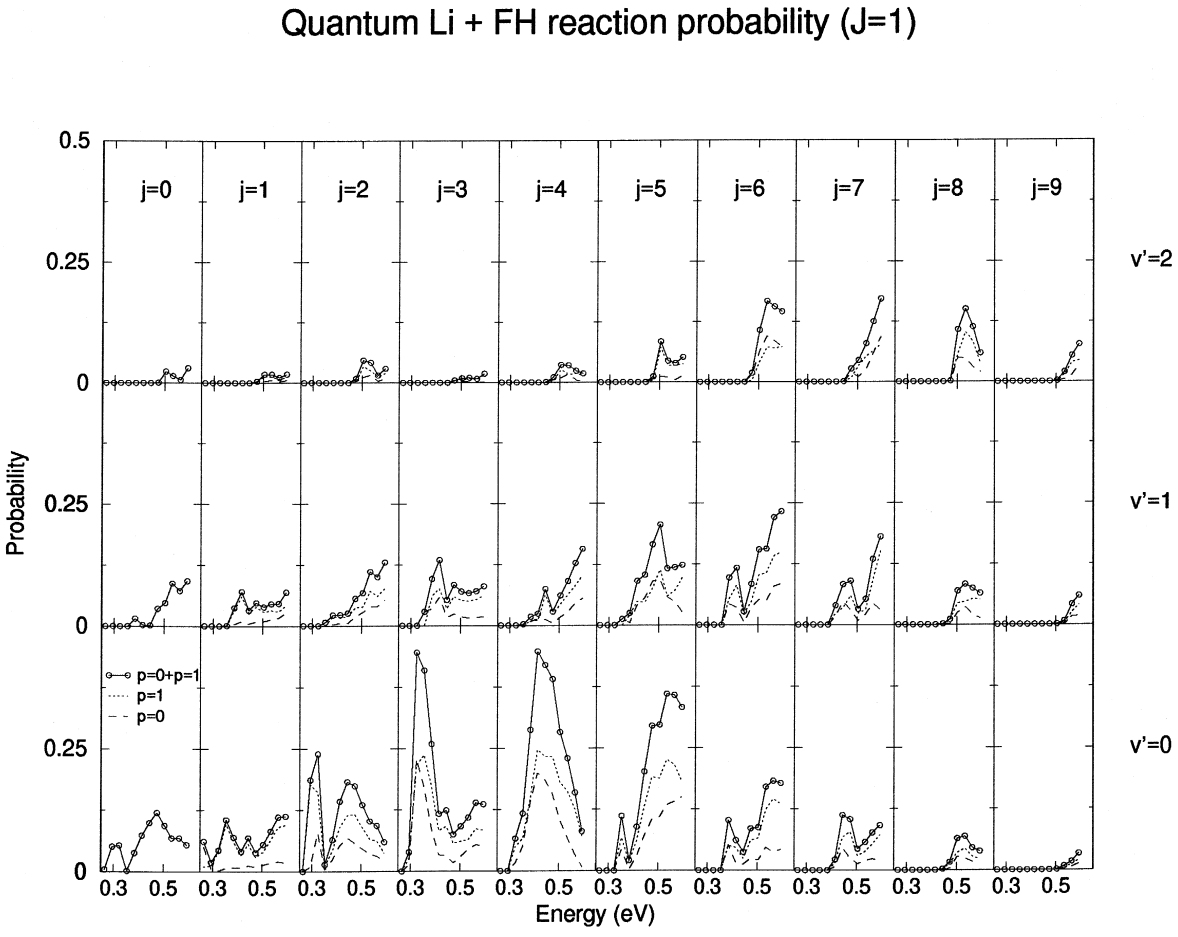

Fig. 2. Reactive probabilities summed over rotational product states (j') for single product vibrational states (v') calculated at $v = 0$ and at j values ranging from 0 to 9 (from lhs to rhs) for $J = 1$ and parity $p = 0$ (dashed line) and $p = 1$ (dotted line) plotted as a function of total energy E. The sum of the probabilities for the two parities is plotted as a solid line with circles.

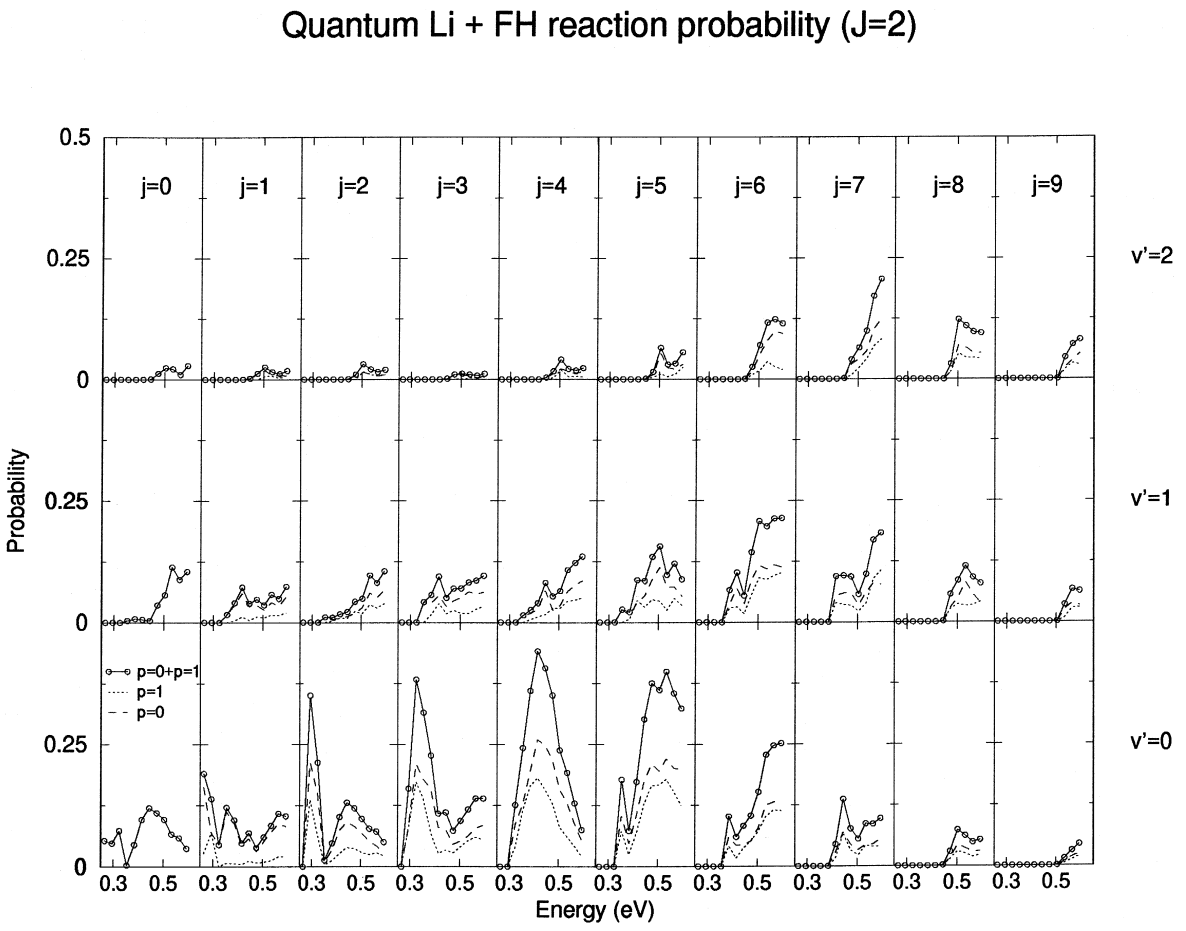

Fig. 3. Reactive probabilities summed over rotational product states (j') for single product vibrational states (v') calculated at $v = 0$ and at j values ranging from 0 to 9 (from lhs to rhs) for $J = 2$ and parity $p = 0$ (dashed line) and $p = 1$ (dotted line) plotted as a function of total energy E. The sum of the probabilities for the two parities is plotted as a solid line with circles.

$J > 0$, $v = 0$ and different j values reactive probabilities are plotted in Fig. 2 for $J = 1$ and in Fig. 3 for $J = 2$. As is apparent from the two figures, the two contributions show the same energy dependence and, apart from a difference in the absolute value (that reflects the different multiplicity of the parities) they have a quite similar behaviour.

4. Cross-sections

To provide a priori estimates of quantities measured in crossed molecular beam apparatuses, reactive probabilities need to weighed and summed over J. This means that fixed J exact quantum calculations need often to be performed at high values of J. However, exact quantum calculations meet increasing computational difficulties as J increases. This is particularly the case of the title reaction proceeding through a strongly bent transition state and not being hydrogen dominated.

For this reason, when calculating high J probabilities approximations are often introduced able to reduce the computational burden. A quite popular approximation that can be used in this case is the so called J-shifting [19,32] approximation. In this approximation the amount of energy associated with the different rotational motion of the whole system

(and therefore with the value of J) is considered to be unavailable for reaction. This allows to set the reactive probability for a given J value equal to that calculated at a different J value provided that energy is scaled accordingly. Since the J shifting approximation is most often applied to $J=0$ reactive probabilities, one can make use of the following relationship

$$P^{J}_{vj,v'j'}(E) = P^{J=0}_{vj,v'j'}(E^{J}) \qquad (6)$$

where $P^{J}_{vj,v'j'}(E)$ is the (estimate of the) state specific probability from the vj vibrotational state to the $v'j'$ vibrotational state at the total energy E and the total angular momentum quantum number J ($P^{J=0}_{vj,v'j'}(E^{J})$) is the square modulus of the state to state **S** matrix element calculated at $J=0$ and an energy E^{J} obtained by subtracting to the total energy E the rotational energy of the triatom evaluated at the geometry of the transition state).

For Li + HF, due to the definite heavy heavy light nature of the system and to the late location of the barrier to products in the exit channel, a further approximation can be introduced by substituting triatomic LiFH rotational energies with diatomic LiF ones. The application of this approximation starting from exact $J=0$ exact quantum probabilities led to satisfactory results as discussed in Ref. [19]. It was found, in fact, that calculated values agree within experimental error bars with measured cross-sections [11]. This is confirmed by the use of the new **S** matrix elements obtained from the revised version of the APH3D computational procedure (see solid line of Fig. 4).

Estimates of the cross-section obtained from a J-shifting approximation can be gradually improved by replacing J shifted probabilities with exact quantum probabilities and by performing the shift using the highest J calculated exact probabilities. In such an improved treatment $P^{J}_{vj,v'j'}(E)$ is, therefore, set equal to the exact state-to-state probability, when this is available. In all other cases, it is estimated by properly shifting the exact state-to-state probability calculated at J^{*} (a reference value of J for which

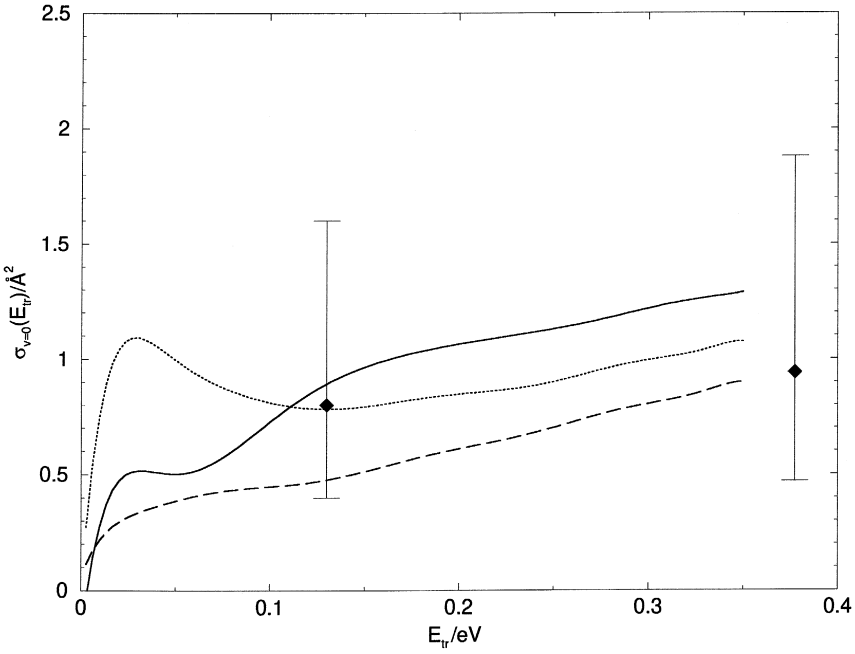

Fig. 4. J-shifting reactive cross-section calculated using the $J=0$ exact quantum probabilities (solid line), the $J=0$ and $J=1$ exact quantum probabilities (dashed line) and the $J=0$, $J=1$ and $J=2$ exact quantum probabilities (dotted line) plotted as a function of translational energy. For comparison, measured values are also reported (diamonds with error bar lines).

exact calculations have been performed). Accordingly, the following relationship

$$P^{J}_{vj,v'j'}(E) = P^{J^*}_{vj,v'j'}(E^{J,J^*}) \quad (7)$$

applies where E^{J,J^*} is set equal to $E - B_{\mathrm{LiF}}(J - J^*)(J - J^* + 1)$ with B_{LiF} being the spectroscopic constant of the LiF diatom. Accordingly, the integral reactive cross-section can be formulated as

$$\sigma_v^{JS}(E_{\mathrm{tr}}) = \sum_j \frac{\pi(2j+1)e^{-\varepsilon_j/k_{\mathrm{B}}T}}{k^2_{vj}Q_{\mathrm{rot}}} \sum_J (2J+1) \times \sum_{v'j'} P^{J}_{vj,v'j'}(E_{\mathrm{tr}}) \quad (8)$$

where, as is typical of experimental data the cross-section has been expressed in terms of the translational energy E_{tr} (rather than in terms of the total energy E).

Using Eq. (8) and exact quantum probabilities for $J = 0$, $J = 1$ and $J = 2$ we calculated the reactive cross-section of the title reaction at initial conditions mimicking the experiment. Related results are plotted in Fig. 4. As already mentioned, the agreement with the measured cross-section when the J-shifting model is applied to $J = 0$ probabilities is, indeed, satisfactory as far as the absolute value is concerned (experimental error bars are estimated by the authors of Ref. [11] to be of the order of 2). However, for the dependence of the cross-section from collision energy the authors of Ref. [11] set stricter boundaries which are not met by the calculations. Yet, when exact quantum probabilities for $J = 1$ (dashed line) and $J = 1$ and $J = 2$ terms (dotted line) are included, and the shifting is performed on the reactive probability curves calculated for non zero J values, the average value of the cross-section in the considered energy interval lowers getting closer to that of the experiment. In addition, while the lowering of the average value of the $J = 1$ results is more dramatic and more evenly distributed, the lowering of the average value of the $J = 2$ results is smaller and more selective. In fact, it penalizes the value of the estimated cross-section in the higher-energy region while increasing that at low energy improving the agreement not only of the absolute value of the cross-section but also of its trend with energy.

Another interesting feature of these results is the surviving in the evaluated cross-section of the low-energy resonant structure characterizing the reactive probabilities after the partial wave averaging. In fact, while in the $J = 1$ results the low-energy structure is almost completely smoothed it becomes clearly apparent when $J = 2$ data are used. Threshold resonance effects have been already discussed in theoretical studies [33] and have obvious effects on the system dynamics and on the rate of the reactive process. The experimental detection of chemical reactive resonances, however, is particularly difficult. Most of the work has concentrated on the $F + H_2$ reaction and its isotopic variants. Theoretical calculations and experiments agree in indicating that the $F + HD$ ($v = 0$, $j = 0,1$) $\rightarrow$ $HF(v', j') + D$ reactive process has a low-energy structure of definite resonant nature [34]. As shown by Fig. 4, the present work suggests that this may be also the case of the Li + HF reaction at the conditions of the crossed molecular beam experiment [11,12] when more low-energy measurements of the reactive cross-section become available.

Obviously, the J-shifting treatment can be further improved not only by pushing the use of exact quantum results to higher J values but also by making more flexible the J-shifting model in terms of the dependence of the average value of the probability from J. Interesting indications in this sense come from plots of quantum probability calculated for the same reaction on a different surface (see Ref. [35]) using a time-dependent method.

5. Conclusions

Exact quantum calculations for the Li + HF reaction have been performed for values of the total angular momentum quantum number differing from zero. From the calculated probabilities it has been possible to evaluate the effect of an increase of the total angular momentum to reaction as well as the role played by the contributions to reactivity from the two parities.

The main aim of this Letter was, however, to investigate whether approximations are able to surrogate exact calculations for high J values. In particular, the validity of using a J-shifting model was investigated by progressively including more contri-

butions from exact quantum probabilities. Although from a comparison of the **S** matrix elements themselves calculated at increasing values of J it was not immediately apparent how effective could be the model, a comparison of reactive cross-sections calculated with an increasing contribution from exact results showed a progressive convergence of the calculated cross-section towards the experimental value. The calculations singled out also another important features of the results. Low-energy values of the integral cross-sections show that there are resonance structures that survive the partial wave averaging.

Acknowledgements

We acknowledge support to this work from EU through COST in chemistry (action D9 project 0003/98) and TMR (contract ERB FMGE CT95 0062 assigned to CESCA-CEPBA and contract ERB FMGE CT95 0051 assigned to EPCC) and from italian MURST, CNR and ASI. We also thank the IFCAI CNR center of Palermo for allowing us to use its computers within the collaborative framework of the PQE2000 project and INFN for a fellowship.

References

[1] A. Riganelli, A. Laganà, in: Lecture Notes in Chemistry, Computational Reaction and Molecular Dynamics: from Simple Systems and Rigorous Methods to Large Systems and Approximate Methods 128 (2000) 1.
[2] P. Casavecchia, Rep. Progr. Phys. 63 (2000) 355.
[3] J.M. Alvariño, P. Casavecchia, O. Gervasi, A. Laganà, J. Chem. Phys. 77 (1982) 6341.
[4] I. Noorbatcha, N. Sathyamurthy, J. Chem. Phys. 77 (1983) 67.
[5] A. Laganà, M.L. Hernández, J.M. Alvariño, Chem. Phys. Lett. 106 (1984) 41.
[6] J.M. Alvariño, M.L. Hernández, E. Garcia, A. Laganà, J. Chem. Phys. 84 (1986) 3059.
[7] A. Laganà, A. Aguilar, X. Gimenez, J.M. Lucas, Chem. Phys. Lett. 189 (1992) 138.
[8] A. Laganà, G. Ochoa de Aspuru, A. Aguilar, X. Gimenez, J.M. Lucas, J. Phys. Chem. 99 (1995) 11696.
[9] M. Baer, I. Last, H.J. Loesch, J. Chem. Phys. 101 (1994) 9648.
[10] A. Aguado, M. Paniagua, M. Lara, O. Roncero, J. Chem. Phys. 107 (1997) 10085.
[11] C.H. Becker, P. Casavecchia, P.W. Tiedemann, J.J. Valentini, Y.T. Lee, J. Chem. Phys. 73 (1980) 2833.
[12] H.J. Loesch, F. Stienkemeier, J. Chem. Phys. 98 (1993) 9570.
[13] G.A. Parker, A. Laganà, S. Crocchianti, R. T Pack, J. Chem. Phys. 102 (1995) 1238.
[14] E. Garcia, A. Laganà, Mol. Phys. 56 (1985) 629.
[15] M.M.L. Chen, H.F. Schaefer, J. Chem. Phys. 72 (1980) 4376.
[16] P. Palmieri, A. Laganà, J. Chem. Phys. 91 (1989) 7303.
[17] G.A. Parker, R. T Pack, A. Laganà, Chem. Phys. Lett. 202 (1993) 75.
[18] F. Gögtas, G.G. Balint-Kurti, A.R. Offer J. Chem. Phys. 104 (1996) 7927.
[19] A. Laganà, G.A. Parker, R.T. Pack, J. Chem. Phys. 99 (1993) 2269.
[20] J.M. Alvariño, V. Aquilanti, S. Cavalli, S. Crocchianti, A. Laganà, T. Martinez, J. Chem. Phys. 107 (1997) 3339.
[21] J.M. Alvariño, V. Aquilanti, S. Cavalli, S. Crocchianti, A. Laganà, T. Martinez, J. Phys. Chem. 102 (1998) 9638.
[22] M.P. de Miranda, S. Crocchianti, A. Laganà, J. Chem. Phys. 103 (1999) 10776.
[23] A. Laganà, A. Bolloni, S. Crocchianti, Phys. Chem. Chem. Phys. 2 (2000) 535.
[24] G.A. Parker, S. Crocchianti, unpublished work.
[25] R.T. Pack, G.A. Parker, J. Chem. Phys. 87 (1987) 3888.
[26] G.A. Parker, R. T Pack, A. Laganà, B.J. Archer, J.D. Kress, Z. Bačic, in: A. Laganà (Ed.), Supercomputer Algorithms for Reactivity, Dynamics and Kinetics of Small Molecules, Kluwer, Dordrecht, 1989, p. 105.
[27] R.T. Pack, G.A. Parker, J. Chem. Phys. 98 (1993) 6883.
[28] J.M. Launay, M. LeDourneuf, Chem. Phys. Lett. 163 (1989) 178.
[29] A. Bolloni, A. Riganelli, S. Crocchianti, A. Laganà, Lecture Notes Comp. Sci. 1497 (1998) 331.
[30] A. Laganà, S. Crocchianti, A. Bolloni, V. Piermarini, R. Baraglia, R. Ferrini, D. Laforenza, Comp. Phys. Comm. xx (1999) xx.
[31] J.M. Alvariño, F.J. Basterrechea, A. Laganà, Mol. Phys. 59 (1986) 559.
[32] J.M. Bowman, J. Chem. Phys. 95 (1991) 4960.
[33] D.G. Thrular (Ed.), Resonances In Electron-Molecule Scattering, van der Waals Complexes, and Reactive Chemical Processes, ACS Symposium Series, vol. 263, 1984.
[34] R.T. Skodje, D. Skouteris, D.E. Manolopoulos, S.-H. Lee, F. Dong, K. Liu, J. Chem. Phys. 112 (2000) 4536.
[35] M. Lara, A. Aguado, O. Roncero, M. Paniagua, J. Chem. Phys. 109 (1998) 9391.